https://doi.org/10.5194/egusphere-2026-3513
Preprint. Discussion started: 13 July 2026

Towards a universal hydrologic metric for predicting rainfall-triggered landslide timing

Jacob B. Woodard[1]; Lisa V. Luna[1]; Benjamin B. Mirus[1]

[1]U.S. Geological Survey, Geologic Hazards Science Center, 1711 Illinois Street, Golden, CO 80401, USA
Correspondence to: Jacob B. Woodard (jwoodard@usgs.gov)

Abstract. Metrics that approximate hillslope hydrologic response to rainfall are fundamental for informing landslide risk reduction efforts, such as early warning systems and hazard models. Notwithstanding the numerous publications using different wetness metrics that underpin and largely control the accuracy of landslide risk reduction products, a robust comparison of a broad array of different wetness metrics for regional landslide analysis is currently lacking in the literature. In this study, we statistically compare common wetness metrics for predicting the temporal occurrence of rainfall-triggered landslides at regional scales (> 1000 km^2) using a landslide inventory covering the contiguous United States. We find that representations of hillslope wetting and drainage using parsimonious leaky bucket models that only require rainfall input and an estimated drainage factor can identify landslide-triggering hydrologic conditions across disparate ecological regions more accurately than unmodified precipitation metrics or more complex hydrological models. Due to the proliferation of global precipitation datasets and the limited input data needed for the parsimonious leaky bucket model, this model could be used to improve tools for landslide risk reduction.

1 Introduction

Rainfall-triggered landslides are widespread and highly destructive natural hazards. Globally, landslides are estimated to cause thousands of deaths (Froude and Petley, 2018; Haque et al., 2019) and substantial property and infrastructure losses every year (Burns et al., 2017; Mirus et al., 2020; National Research Council, 1985). Consequently, the development of landslide risk reduction products (e.g., hazard models and early warning systems) that effectively characterize the initiation potential of rainfall-triggered landslides consistently and accurately over large regions (> 1000 km^2) is of primary importance (Godt et al., 2022). These landslide risk reduction products generally assess both spatial and temporal variability in landslide hazard (Dahal et al., 2024; Felsberg et al., 2023; Moreno et al., 2024; Stanley et al., 2021; Steger et al., 2022). Hundreds of studies have looked exclusively at the spatial component, or susceptibility, of risk reduction products (Reichenbach et al., 2018), such that the methods for estimating the spatial variability in landslide hazard are well-informed. However, fewer studies have focused on evaluating different methods for estimating the temporal component of rainfall-triggered landslide risk reduction products, leaving modelers with little guidance on how to effectively characterize temporal changes in hazard in regional analysis. Importantly, the temporal component is often the primary discriminating factor of landslide potential over landslide-prone regions (Mondini et al., 2023).

https://doi.org/10.5194/egusphere-2026-3513
Preprint. Discussion started: 13 July 2026

Rainfall that infiltrates the soil can cause pore-water pressures to increase within the hillslope, which decreases the hillslope's resistive stress and increases its potential to fail (e.g., Lambe and Whitman, 1979). The complex interaction between infiltration and drainage that controls pore-water pressures is difficult to predict due to the heterogeneous and poorly constrained subsurface properties that control water behavior within hillslopes. It follows that water pressures at any given time are controlled not only by the current rainfall conditions, but also by the antecedent conditions leading up to the present. Consequently, foundational to any landslide risk reduction efforts are a wetness metric that captures the influence of recent and antecedent rainfall on hillslope hydrology (Crozier, 1999; Okada et al., 2001; Wilson and Wieczorek, 1995).

The proliferation of water-related datasets that estimate rainfall or soil moisture and multitemporal landslide inventories has led to a corresponding increase in landslide wetness metrics that attempt to meet the demand for more reliable regional-scale risk reduction products. These metrics include empirical thresholds based on either intensity-duration (ID) thresholds (e.g., Guzzetti et al., 2008) or hydrometeorological conditions (e.g., Bogaard and Greco, 2018), physics-based approaches (e.g., Baum et al., 2010), and complex land surface models (LSMs) driven by multiple satellite-based observations (e.g., Reichle et al., 2017, 2025).

Empirical rainfall-based threshold methods are the most used class of metric for assessing rainfall-triggered landslide potential (Brunetti et al., 2010; Caine, 1980; Guzzetti et al., 2008; Saito et al., 2010; Segoni et al., 2018b). This is due, in part, to their simplicity, access to requisite datasets, and their effectiveness in some applications, such as in local watersheds with sufficient data to constrain the threshold. Empirical threshold approaches involve using past landslide observations to segregate landslide-triggering conditions from non-landslide-triggering conditions. However, this class of metrics does not account for the variable intensity of longer-duration storms, the antecedent soil moisture conditions, or the heterogeneous hillslope properties that can cause optimal thresholds to change temporally and spatially (Bogaard and Greco, 2018; Mirus et al., 2018, 2025).

Physics-based metrics have the advantage of being able to more accurately simulate the non-linear responses of pore-water pressures to rainfall, provided accurate boundary conditions and parameter estimates (Baum et al., 2008; Dietrich and Montgomery, 1998; Ebel et al., 2008; Iverson, 2000; Mathews et al., 2024; Pack, 1998). However, these approaches are most effective when informed by comprehensive datasets that characterize the hydrological and geomechanical conditions of individual hillslopes, which vary widely across landscapes. Over regional or greater scales, the collection of these data at sufficient detail to achieve accurate results is currently unfeasible. Consequently, some simplified physics-based models have been proposed that reduce the input data needs (Okada et al., 2001; Perkins et al., 2025; Saito and Matsuyama, 2012; Wilson and Wieczorek, 1995), but these come with a loss of physical basis and local precision.

Modern satellite observations have given rise to new estimates of soil hydrologic state variables, such as soil-water content based on complex LSMs. These LSMs estimate the water and energy fluxes between atmospheric, surface,

https://doi.org/10.5194/egusphere-2026-3513
Preprint. Discussion started: 13 July 2026

and subsurface systems while driving the model with satellite and other earth-system datasets. Examples of these efforts include the soil moisture active passive (SMAP) mission (Reichle et al., 2017, 2025), the National Oceanic and Atmospheric Administration's national water model (NWM) (Cosgrove et al., 2024), and the European Centre for Medium-Range Weather Forecasts Reanalysis (ERA-5) product (Muñoz-Sabater et al., 2021). The output of these models includes estimates of soil moisture at variable depths. These approaches have garnered widespread attention in the landslide sciences and have been used to inform criteria for landslide early warning systems (Palazzolo et al., 2025) and hazard models (Felsberg et al., 2023). However, these products were not designed to explicitly estimate the complex wetting and drainage dynamics in steeper hillslopes (Thomas et al., 2019). Additionally, their imprecise data inputs (e.g., Fan et al., 2022; Reichle et al., 2017), simplified governing equations for estimating groundwater flux, and coarse spatial resolutions raise concerns about their utility in quantifying hillslope hydrology for slope stability assessments (Thomas et al., 2019).

Few studies have attempted to systematically compare the effectiveness of differing wetness metrics for landslide prediction over heterogeneous regions. Felsberg et al. (2023) evaluated the antecedent rainfall index used in the first version of the Landslide Hazard Assessment (LHASA) model against daily rainfall, the SMAP estimates of soil moisture at one-meter depth, and a combination of rainfall and soil moisture. They found that the metric that combines rainfall and soil moisture performed the best on their global dataset. Marc et al. (2018) evaluated peak 3-hour rainfall intensity, total storm accumulation, and storm duration with eight rainfall-triggered landslide inventories across the world and found that total storm accumulation was the most predictive metric for landsliding. Godt et al. (2006) and Perkins et al. (2025) evaluated different parameterizations of a simple leaky-bucket model to simulate the processes of infiltration and drainage. A leaky bucket model, in its simplest form, uses a mass balance paradigm where rainwater is added to a reservoir that drains at a rate proportional to the reservoir level (Wilson and Wieczorek, 1995). The reservoir level is used as a proxy of hillslope wetness that reflects the storage dynamics in response to infiltration and drainage processes. Godt et al. (2006) tested a slightly more advanced leaky bucket model in combination with a rainfall intensity-duration threshold over the U.S. city of Seattle, Washington, whereas Perkins et al. (2025) applied a recurrence-interval-based leaky bucket model across the U.S. state of California. They both found that this simple approach could effectively differentiate between landslide and non-landslide triggering hydrologic conditions (Crozier, 1999). All of these studies focused primarily on method development and proof of concept for local or regional study areas, rather than on comparing the validity and practical implementation of multiple contrasting approaches across broad areas.

A fundamental challenge of all wetness metrics is how to account for the local conditions that affect pore-water dynamics at the location of landslide initiation. Local conditions such as the physical properties of soils, soil depth, vegetation, and soil layering can all affect pore-water dynamics and are highly heterogeneous, especially at regional scales (Mirus, 2015; Pelletier et al., 2016; Richardson et al., 2019; Schmidt et al., 2001). Furthermore, these data are generally unavailable with sufficient detail to be accounted for explicitly across broad areas. One method of mitigating the effects of these heterogeneous conditions is converting the wetness metrics into statistical measures of

https://doi.org/10.5194/egusphere-2026-3513
Preprint. Discussion started: 13 July 2026

abnormality that account for the long-term wetness patterns of a given location (Felsberg et al., 2023; Marc et al., 2019, 2022; Okada et al., 2001; Perkins et al., 2025; Saito and Matsuyama, 2012; Tsunetaka, 2021; Wilson and Jayko, 1997). This conversion can be done by turning the wetness metrics into percentiles at a given location (Felsberg et al., 2023) or normalizing by the value of the metric at a given recurrence interval at a given location (e.g., 10-year event) (Marc et al., 2019; Okada et al., 2001; Perkins et al., 2025; Saito and Matsuyama, 2012). Converting the wetness metrics into spatial abnormalities can better distinguish landslide-triggering precipitation events from non-landslide-triggering events, presumably because landscapes are conditioned to the local environment (Emberson et al., 2022; Marc et al., 2018, 2019; Milledge et al., 2019; Woodard and Mirus, 2025). This local tuning results in landslides generally occurring under relatively extreme hydrologic conditions, which may not be consistent across an area of interest.

An understanding of the efficacy of differing wetness metrics for regional-scale landslide prediction is currently lacking. Consequently, there is little guidance on which wetness metrics should be used in regional-scale landslide risk reduction products. In this study, we address this knowledge gap by statistically evaluating the ability of 15 different wetness metrics to discriminate between landslide-triggering and non-landslide-triggering hydrologic conditions over broad and disparate regions of the United States. These metrics were designed to facilitate implementation over regional scales with data that is available over the contiguous United States (CONUS). We show that the parsimonious leaky bucket metrics have the best overall discriminating power across diverse ecological regions. This added understanding of the most effective wetness metrics for predicting the timing of rainfall-triggered landslides may facilitate the creation of more robust landslide risk reduction products. This improvement, in turn, could provide actionable information to help protect communities from landslide-associated losses.

2 Materials and Methods

We compare 15 different wetness metrics for landslide initiation potential that have been used with success in other studies (Table 1). From the least to the most complex, these include 24-hour precipitation totals, daily maximum hourly precipitation totals (max hourly precipitation), antecedent rainfall index (ARI) (Kirschbaum and Stanley, 2018), six parameterizations of an antecedent wetness index (AWI) (Wilson and Wieczorek, 1995), two parameterizations of a physics-based transient rainfall infiltration (TRI) model (Baum et al., 2008, 2010; Iverson, 2000), the national water model (NWM) (Cosgrove et al., 2024), the soil moisture active-passive (SMAP) (Reichle et al., 2025), and two metrics that combine precipitation and the SMAP soil moisture estimates. One important consideration in making the wetness metrics appropriate for regional-scale analysis is the input data requirements (Table 1). The TRI models have the most user input data requirements, and the two LSM-based models (NWM and SMAP) have the fewest user input data requirements. The data latency, resolution, and coverage for most of the metrics are dictated by the data used as dynamic user inputs for all the metrics except the NWM and SMAP metrics. We provide these data details in section 2.1.

https://doi.org/10.5194/egusphere-2026-3513
Preprint. Discussion started: 13 July 2026

Table 1. Wetness metrics overview. Metric acronyms and constants are defined as follows: ARI - antecedent rainfall index; AWI - antecedent water index; kd - a drainage constant; TRI - transient rainfall index; NWM - national water model; SMAP - soil moisture active-passive.

Wetness Metric	Dynamic User Inputs	Static User Inputs
24-hour precipitation	Daily precipitation	None
Max hourly precipitation	Hourly precipitation	None
ARI	Daily precipitation	None
AWI: kd = 0.001	Daily precipitation	Drainage constant
AWI: kd = 0.01	Daily precipitation	Drainage constant
AWI: kd = 0.1	Daily precipitation	Drainage constant
AWIET: kd = 0.001	Daily precipitation	Drainage constant, uniform field capacity, mean evapotranspiration rates
AWIET: kd = 0.01	Daily precipitation	Drainage constant, uniform field capacity, mean evapotranspiration rates
AWIET: kd = 0.1	Daily precipitation	Drainage constant, uniform field capacity, mean evapotranspiration rates
TRI: variable	Daily precipitation	Spatially varying specific storage and saturated hydraulic conductivity, mean evapotranspiration rates
TRI: uniform	Daily precipitation	Spatially uniform specific storage and saturated hydraulic conductivity, mean evapotranspiration rates
NWM	None	None
SMAP	None	None
SMAP + daily precipitation	Daily precipitation	None
SMAP + max hourly precipitation	Hourly precipitation	None

2.1 Data

The data processing in this study is conducted in R (R Core Team, 2025) and Python (Python Software Foundation, 2025) with computation assistance from the U.S. Geological Survey (USGS) supercomputer, Hovenweep (Falgout et al., n.d.). All spatial datasets are converted to a World Geodetic System (WGS) 84 projection. Temporal datasets are converted to the Coordinated Universal Time (UTC), trimmed to cover a temporal range of March 31, 2015, through December 31, 2022, and spatially limited to CONUS to ensure consistent coverage between all the datasets. For the metrics that account for antecedent rainfall, including the antecedent rainfall index (ARI), antecedent water index (AWI), and transient rainfall index (TRI) metrics, we allowed the models to ramp up to the March 31, 2015 date by running the model for the preceding year starting with an initial metric value of zero before temporally trimming it to match the other datasets.

2.1.1 Landslide inventory

The landslide occurrence data used in this study are from Version 3 of the USGS compilation of landslide

https://doi.org/10.5194/egusphere-2026-3513
Preprint. Discussion started: 13 July 2026

inventories across the United States (Belair et al., 2025). Disparate inventories included in this compilation come from a variety of different sources that use different methodologies for mapping and cataloging landslides as points or polygons (Mirus et al., 2020); the USGS integrates these disparate inventories into a database with uniform attributes, including estimates on reported landslide timing (Belair et al., 2025). We convert all polygon-mapped landslides to points by selecting their centroids. We only include landslides with daily or better temporal precision. Finally, because we are only interested in rainfall-triggered landslides, we remove earthquake-triggered landslide inventories and landslides with zero observed precipitation on the failure day. We remove any duplicate landslide points from the inventory by comparing the spatial extents and timing of the mapped landslides. Additional landslide attributes such as size, depth, or type of movement (Varnes, 1978) were not analyzed because this information is not reported consistently for most of the landslides in the inventory. When extracting attributes of the landslides from other datasets (i.e., precipitation (section 2.1.2), soil parameters (section 2.1.3), and evapotranspiration (2.1.4)), we extract the data cell that is geographically closest to the landslide point. Some of the other datasets had null values at a few landslide locations; we also removed these landslides to ensure a consistent comparison between the wetness metrics. The final number of landslides used for this analysis is 1,790, and they are distributed across CONUS with widely varying elevations, mean annual precipitation, and ecoregions (Figure 1).

https://doi.org/10.5194/egusphere-2026-3513
Preprint. Discussion started: 13 July 2026

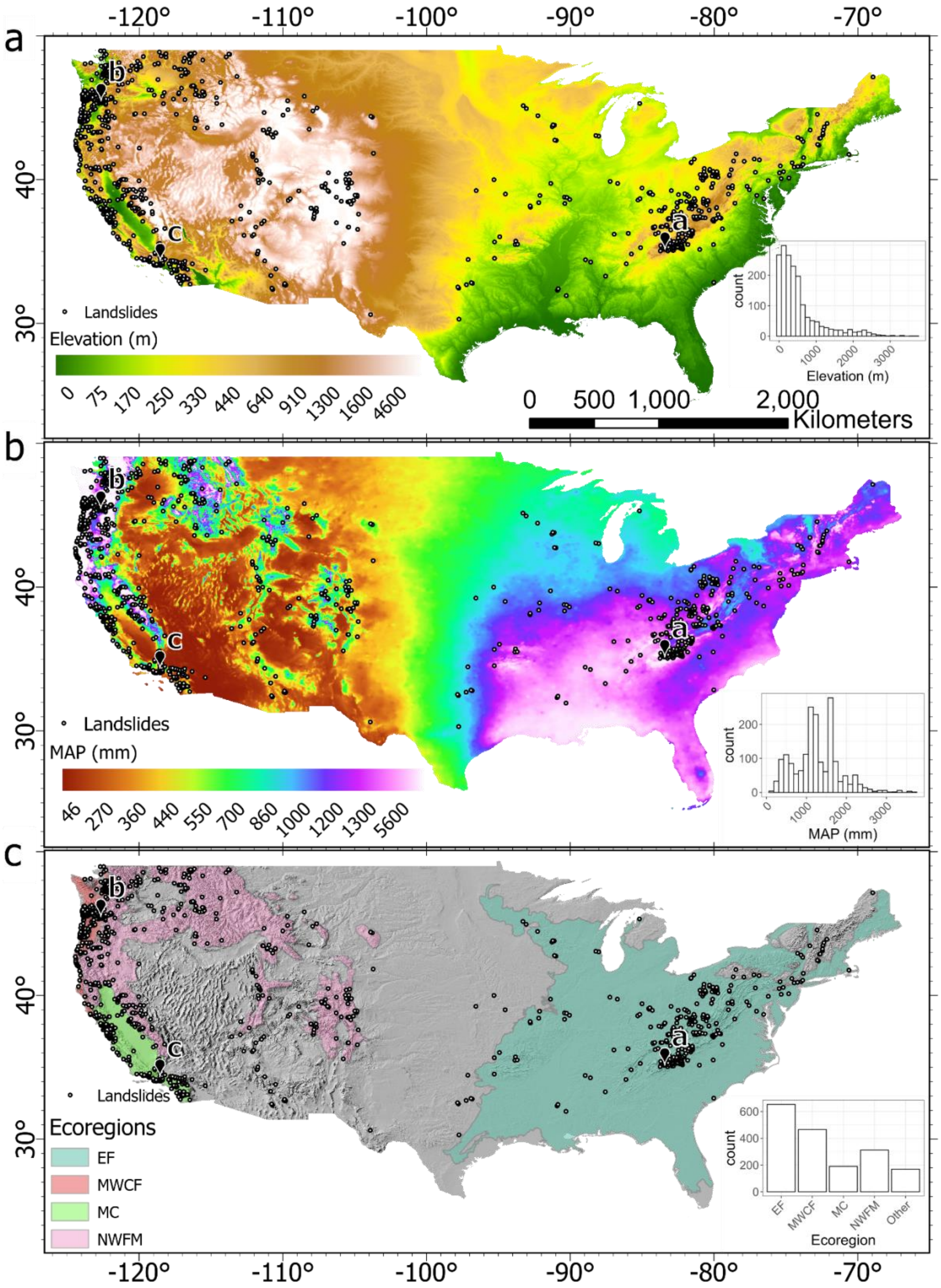

175

https://doi.org/10.5194/egusphere-2026-3513
Preprint. Discussion started: 13 July 2026

Figure 1: (a) Elevation (U.S. Geological Survey, 2018), (b) mean annual precipitation (MAP) (PRISM Climate Group, 2019), and (c) level-one ecoregions (Omernik and Griffith, 2014) over the contiguous United States. The white dots show the subset of landslide locations from Belair et al. (2025) that are used in this analysis. Black pins show the landslide point locations selected for the time series in Figure 4. Ecoregions represented are the Eastern Temperate Forests (EF), Marine West Coast Forest (MWCF), Mediterranean California (MC), and Northwestern Forested Mountains (NWFM). Histograms in each subfigure show the landslide counts for each parameter class.

2.1.2 Precipitation estimates

We use the analysis of record for calibration (AORC) dataset produced by NOAA for precipitation totals at the landslide locations (Fall et al., 2023; NOAA, 2025). There are many different precipitation datasets, all with their advantages and disadvantages (Schneider et al., 2013). We select the AORC dataset because of its high spatial (~800 m) and temporal (one hour) resolutions, long temporal record (since 1979), spatial coverage over the CONUS, and easy-to-use data format (zarr). The AORC estimates hourly precipitation by disaggregating the more reliable monthly precipitation estimates into daily and hourly estimates using less constrained datasets with higher temporal resolutions (Fall et al., 2023; NOAA, 2025). The AORC largely relies on radar and daily precipitation gauge observations (Du, 2011; Lin and Mitchell, 2005), which have been the standard for comparing other precipitation datasets due to their high accuracy (Beck et al., 2019). Some of the notable weaknesses of the AORC dataset include spurious high precipitation data, regional biases caused by the precipitation gauge infrastructure, and not differentiating precipitation types (i.e., rain versus snow). We assume that the precipitation-triggering conditions in our landslide inventory are caused by rainfall. We convert the precipitation units from mass per area ($\mathrm{kg/m^2}$) to meters of rainfall by dividing by the density of water (1000 $\mathrm{kg/m^3}$). The AORC dataset has a latency of 10 days to permit the inclusion of the gauge data.

2.1.3 Soil Parameters

The two TRI models require estimates of the specific storage ($S_s; m^{-1}$) and saturated hydraulic conductivity ($K_s; m/day$). These parameters are extracted from California Soil Resource Laboratory's (Walkinshaw et al., 2023) rasterized version of the soil survey geographic database (SSURGO) (U.S. Department of Agriculture, 2021a) and state soil geographic database, version 2 (STATSGO2) (U.S. Department of Agriculture, 2021b) databases. The SSURGO dataset is a compilation of soil characteristics of the United States developed from field surveys and laboratory tests. Data are collected at scales ranging from 1:12,000 to 1:63,360. Locations missing SSURGO data are filled in using the STATSGO2 dataset. The STATSGO2 dataset is mapped at a coarser resolution of 1:250,000 over most of the CONUS. The final rasters have a spatial resolution of 800 m and area only available over CONUS. The S_s is approximated using the available water holding capacity (AWC; m/m). Refer to supplemental text S1 for details on this relationship.

https://doi.org/10.5194/egusphere-2026-3513
Preprint. Discussion started: 13 July 2026

2.1.4 Evapotranspiration

Some of the AWI parameterizations and the TRI metrics require estimates of an evapotranspiration rate constant ($V; m/hr$) at each landslide location. We extract these values from Reitz et al. (2023) by taking the mean hourly evapotranspiration rate from 2010 to 2018. These data have an 800 m spatial resolution and combine water balance, field observations (flux towers), and remotely sensed estimates to determine the evapotranspiration rates.

2.2 Wetness metrics

2.2.1 Precipitation metrics

We evaluate three different precipitation metrics for predicting landslide days. The first two are raw (unmodified) precipitation totals of different durations: daily accumulation (referred to as 24-hour precipitation) and daily maximum one-hour precipitation intensity (referred to as max hourly precipitation). We also evaluate the ARI metric used by Kirschbaum and Stanley (2018) which is parameterized as follows:

$$ARI = \frac{\sum_{t=0}^{6} I_t w_t}{\sum_{t=0}^{6} w_t}, \tag{1.1}$$

$$w_t = (t+1)^{-2}. \tag{1.2}$$

This metric takes into account the rainfall of the preceding week using a weighting function (w_t) that gives the most weight to total precipitation ($I_t; m$) during the time interval ($t; day$) closest to the present day ($t = 0$). Any number of time windows could be used for these precipitation metrics. However, the three chosen here cover common intervals to predict landslides (Segoni et al., 2018a). These precipitation metrics benefit from not requiring any additional parameters and are among the simplest metrics evaluated in this study.

2.2.2 Antecedent water indices

We apply two versions of the leaky bucket model that estimate the antecedent water index (AWI; m) as a proxy for the hydrologic response to rainfall. These are simple physics-based methods that estimate the non-linear decay in soil moisture using a reduced number of parameters compared to physics-based models. The basis of these models was developed by Wilson and Wieczorek (1995) and later adopted by Godt et al. (2006) and Perkins et al. (2025). The first version of the AWI metric ignores evapotranspiration and the linear AWI build-up before reaching the soil's field capacity and is calculated as follows:

$$AWI_t = AWI_{t-1}e^{-k_d\Delta t} + \frac{I_m}{k_d}(1 - e^{-k_d\Delta t}), \tag{2}$$

where I_m is the mean precipitation intensity measured during time t (m/hr), k_d is a drainage constant that controls

https://doi.org/10.5194/egusphere-2026-3513
Preprint. Discussion started: 13 July 2026

the decay rate of AWI following a precipitation event (h^{-1}) and Δt is the time increment (24-hr). In the second version, drainage does not occur until the field capacity of the soil is reached and evapotranspiration is considered. This parameterization accounts for capillary flow in addition to gravitational flow, which can improve estimates of the hydrologic response to rainfall within soils (e.g., Godt et al., 2006; Thomas et al., 2019; Wilson and Jayko, 1997). As with previous applications of AWI, we assume field capacity is reached when the soil column accumulates a water depth of 0.18 m, while considering the constant flux of water out of the system due to evapotranspiration. The depth of 0.18 m is the approximate amount of water to bring a 1-meter-thick column of loamy soil to field capacity (Godt et al., 2006; Perkins et al., 2025). We do not attempt to spatially vary the field capacity value due to its poor constraints over CONUS, instead selecting to use a constant value that has been used successfully in other studies (Godt et al., 2006; Perkins et al., 2025). Once that depth is reached, the AWI considering evapotranspiration (AWIET) is modeled as follows:

$$AWIET_t = \begin{Bmatrix} AWI_{t-1}e^{-k_d\Delta t} + \frac{E_t}{k_d}\left(1 - e^{-k_d\Delta t}\right) & E_t > 0 \\ AWI_{t-1}e^{-k_d\Delta t} + E_t\Delta t & E_t \leq 0 \end{Bmatrix}, \tag{3.1}$$

$$E_t = I_m - V, \tag{3.2}$$

where V is the mean evapotranspiration rate (m/hr), and E_t is the effective precipitation rate (m/hr). Following Perkins et al. (2025), we evaluate the AWI and AWIET metrics using three k_d values: 0.1, 0.01, and 0.001 hr^{-1} and 24-hour precipitation totals. Higher k_d values result in faster decay of AWI (Figure S1). Comparison of the AWI metric using hourly and daily precipitation totals shows negligible differences (Figure S2). The AWI metric only requires estimates of precipitation and a drainage constant, making it among the simplest of the modeled metrics evaluated here. The AWIET requires these inputs with the additional static inputs of field capacity and an evapotranspiration constant.

2.2.3 Transient rainfall infiltration

We evaluate a transient rainfall infiltration (TRI) model designed to approximate solutions to Richards' equation (Richards, 1931) derived by Iverson (2000) for the Darcian flow of groundwater in response to rainfall. This model provides a more complex approach for modeling the hydrologic conditions that lead to landsliding compared to the AWI metrics. We adjust the equations for calculating TRI developed by Iverson (2000) and Baum et al. (2008, 2010) to facilitate their application for regional hydrologic response over long periods, as follows:

$$\Omega(t) = 2\sum_{n=1}^{N-2}\frac{I_n}{K_s}\left\{H(t - t_{n+1})\left(D_1(t - t_{n+1})\right)^{\frac{1}{2}}\,\mathrm{ierf}\left[\frac{1}{2\left(D_1(t - t_{n+1})\right)^{\frac{1}{2}}}\right]\right\} \tag{4.1}$$

https://doi.org/10.5194/egusphere-2026-3513
Preprint. Discussion started: 13 July 2026

$$-2\sum_{n=1}^{N-2}\frac{I_n}{K_s}\left\{H(t-t_{n+2})\left(D_1(t-t_{n+2})\right)^{\frac{1}{2}}\,\mathrm{ierf}\left[\frac{1}{2\left(D_1(t-t_{n+2})\right)^{\frac{1}{2}}}\right]\right\}$$

$$-\sum_{n=1}^{N-2}V_n\;H(t-t_{n+2}),$$

$$D_1=\frac{K_s}{S_s}, \tag{4.2}$$

$$\mathrm{ierfc}(\eta)=\frac{1}{\sqrt{\pi}}e^{-\eta^2}-\eta\;\mathrm{erfc}(\eta), \tag{4.3}$$

where Ω(t) is the TRI metric (m) at time t *(day)*, *N* is the total number of time steps, I_n is the precipitation intensity for the n^{th} time step (m/day), H is the Heaviside step function, erfc is the complementary error function, V is the mean evapotranspiration rate (m/day), S_s is the specific storage (1/m), and K_s is the saturated hydraulic conductivity (m/day). This one-dimensional model assumes only vertical flow, water flux at the ground surface, uniform soil properties down to an infinite depth, no surface runoff, that the soils are at field capacity, that the water table is initially at unit depth, and that the TRI metric begins at zero ($\Omega(0)=0$). Furthermore, we assume that the background flux out of the system is equal to the long-term evapotranspiration rates at the modeling location. This background flux acts as a correctional factor to prevent the gradual increase in water pressure that occurs when modeling over long time intervals due to the summation of many erfc functions (eq. 1.3) through time. The original equations by Iverson (2000) and Baum et al. (2008) are designed to estimate the water-pressure head at the assumed depth of failure during a rainfall event. However, accurate assessments of the water-pressure head require accurate boundary conditions that are not feasible to generate over regional scales or for continuous simulation. Our formulation reduces the number of free parameters required by the model but limits us to using Ω as a proxy for the changes in water-pressure head at most reasonable depths for shallow landslides (0.5-10 m) rather than directly estimating this value. We run the TRI model at each landslide location using two different parameter schemes to evaluate the effects of more specific soil parameters on model performance: 1) the best estimates of soil parameter values across CONUS (refer to section 2.1.3) (we refer to this metric as TRI: variable); 2) using uniform soil parameters across space by taking the average parameter values over all the landslide locations (referred to as TRI: uniform). For both TRI wetness metrics (TRI:variable and TRI:uniform), we use spatially varying but temporally constant estimates of V (refer to section 2.1.4). The TRI metrics only require estimates of precipitation as the dynamic user input, but they have the most static user inputs of all the metrics we evaluate (Table 1).

2.2.4 National Water Model

To determine if more complex LSMs can capture the hydrologic conditions that lead to landsliding, we evaluate the

https://doi.org/10.5194/egusphere-2026-3513
Preprint. Discussion started: 13 July 2026

national water model's (NWM) v.3.0 estimates of soil moisture (m^3/m^3) by the National Oceanic and Atmospheric Administration (NOAA) (Cosgrove et al., 2024). The NWM develops forecasts and retrospective estimates of soil moisture and other hydrologic parameters over CONUS at a 1 km spatial resolution and three-hour temporal resolution. The LSM used in the NWM incorporates dynamic drivers, including precipitation, near-surface air temperature, specific humidity, shortwave and longwave radiation, to simulate processes pertinent to hydrology like canopy energy exchange, snowpack, runoff, infiltration, groundwater dynamics, vegetation patterns, and more. The LSM static inputs include soil, vegetation, land use, and other parameters, but these are all prescribed by the model, not the user. The NWM estimates soil moisture at four different depth horizons of variable thicknesses for a total depth of two meters. We take the maximum daily weighted average of these horizons to be our representative daily wetness metric value across the entire time series, using horizon thickness as the weights. The NWM represents one of the more complex models available for evaluating soil moisture. We use the retrospective NWS dataset v3.0 (NOAA, n.d.), which provides estimates of soil moisture between February 1, 1970, and February 2, 2023.

2.2.5 SMAP

We use the soil moisture active-passive (SMAP) satellite-based estimates of root-zone (top 1 m; L4_SM) soil moisture (m^3/m^3) as an alternative example of a complex hydrological model (Reichle et al., 2025). In contrast to the NWM, the SMAP L4-SM algorithm estimates soil moisture from microwave emission and radar backscatter data assimilated into an LSM with 9 km resolution. The SMAP LSM also incorporates many of the same parameters used in the NWM to estimate the flux of water and energy in and out of the root zone reservoirs. Like the NWM, the SMAP algorithm is complex and represents a state-of-the-art data assimilation algorithm for estimating soil moisture. The SMAP soil moisture product requires no user input, has a temporal resolution of 3 hours, global coverage, a seven-day latency, and observations beginning in March 2015.

We evaluate the SMAP soil moisture independently and in combination with precipitation to identify landslide days. We combine precipitation with soil moisture estimates because this has been shown to improve the prediction of landslide events compared to only using soil moisture estimates due to SMAPs low sensitivity to discrete precipitation events (Felsberg et al., 2023; Thomas et al., 2019). Additionally, the newest LHASA model (LHASA 2.0) trains its machine learning model on both rainfall and SMAP soil moisture estimates, motivating us to compare this wetness metric with possible alternatives (Stanley et al., 2021). We extract the maximum daily wetness metric value as representative of landslide failure conditions. We combine soil moisture (M) (m_{water}^3/m_{bulk}^3) estimates with estimates of precipitation (R) (m_{water}) by considering a unit volume of soil and assuming uniform precipitation over that volume (m_{water}^3). Hence, precipitation can be added directly to soil moisture to create a new wetness metric with consistent units (m^3/m^3). We combine two precipitation metrics with the SMAP estimates of soil moisture: the maximum daily one-hour precipitation (SMAP + max hourly precipitation) and the total daily accumulation (SMAP + daily precipitation).

2.3 Conversion to percentiles

For landslide prediction, we define the best wetness metric as one whose values most effectively segregate days with greater than zero precipitation that trigger landslides (i.e., landslide-triggering precipitation days) from non-landslide-triggering precipitation days. Common measures of discriminatory ability include receiver operator characteristics (ROC), precision-recall curves, the Brier score, and many more. However, these metrics rely on complete landslide inventories that accurately reflect the timing and location of events and non-events. An alternative approach is to convert a wetness metric at a specific landslide location to a percentile of days with a total precipitation greater than zero and then take the mean of the percentiles on landslide days across the area of interest. That is, we take the wetness metric time series from a landslide location, subset the time series to only include days with some precipitation recorded, transform this subset of the wetness metric time series into percentiles, and extract the percentile of the landslide day at that location. We do this for all landslide locations within the area of interest and take the mean of the landslide-day percentiles. The conversion of raw metric to percentiles is carried out separately at each landslide location as follows:

$$P_n = 100 * \left(\frac{\varphi_n}{N_w}\right), \tag{5}$$

where P_n is the metric percentile of the timestep n, φ_n is the ordinal rank of the metric value at timestep n, and N_w is the total number of time steps with a total precipitation accumulation value greater than zero. We then take the mean of the percentiles on landslide days as follows:

$$\mu_m = \frac{1}{n_{LS}} \sum_{i=1}^{n_{LS}} P_{LS_i}. \tag{6}$$

Here, μ_m is the mean percentile of landslide days for the wetness metric m, n_{LS} is the number of landslides over the area of interest, and P_{LS} is the metric percentile of the landslide day (Equation 5). The mean of the percentiles of landslide days is measured on each wetness metric individually to permit a comparison of the metrics' discrimination ability between landslide-triggering and non-landslide-triggering rainfall.

A wetness metric that has uniformly high percentiles on landslide days will, by definition, also have a high discriminatory capability. That is, it will have fewer false positives (FP) and false negatives (FN) and more true positives (TP) and true negatives (TN) compared to metrics with lower percentile values. In the supplemental text S2, we demonstrate that in problems where the events of interest are rare compared to non-events, as in the case of temporal landslide inventories, the area under the receiver operator characteristic curves (AUCROC) produced using complete inventories (i.e., true data) is approximately equal to the mean of the event percentiles (refer to

https://doi.org/10.5194/egusphere-2026-3513
Preprint. Discussion started: 13 July 2026

supplemental text S2). The AUCROC compares the recall (TP/(TP+FN)) against the false positive rate (FP/(FP+TN)) at different metric thresholds. The AUCROC metric is among the most popular to validate landslide models due to its ability to effectively communicate the discriminatory ability of the model being tested, even for imbalanced datasets (He and Ma, 2013). We also show in Figure S3 that the top performing wetness metrics using AUCROC are also the top performing metrics using precision (TP/(TP+FP)) recall AUC values, which prioritizes the correct classification of the events over the non-events (Davis and Goadrich, 2006; He and Ma, 2013). The mean of the landslide-day percentile distributions, therefore, serves as an indicator of discriminatory capability that considers any skew towards lower values within the distributions. The ideal metric is one with less skew and percentile values of landslide days concentrated near one. In contrast to other commonly used measures of discriminatory ability, the mean of the landslide-day percentiles does not need a complete inventory; rather, the landslide events analyzed only need to be representative of the triggering events that generally produce landslides. This is because landslide events not included in our inventories do not affect the percentiles of the events we have; they only act to include more observations that are considered for calculating the mean. Consequently, if our inventory is not biased towards more or less extreme precipitation events than those that typically trigger landslides, it does not matter that we have an incomplete inventory. In summary, a higher mean metric percentile of landslide days indicates better discriminatory ability between landslide and non-landslide-triggering precipitation days, and this metric can produce reliable evaluations of metric performance without needing a complete landslide inventory.

The use of percentiles converts the metrics into measures of local abnormality. That is, the higher the percentile, the more extreme the metric value is compared to the median metric values at a specific location. Hence, the use of percentiles as our performance indicator also incorporates the benefits of analyzing metrics in terms of abnormality as described in Section 1.

2.4 Statistical evaluation

We use a Bayesian statistical model to analyze the differences in means of the metric percentile distributions of all landslide days. The limited number of observations in the dataset (refer to section 2.1.1) necessitates a statistical analysis to determine the magnitude of differences between the metrics and to evaluate if any differences are statistically credible. “Credible” is the preferred Bayesian term analogous to “significant” in frequentist statistics (Kruschke, 2015). We develop a model in the software Stan (Stan Development Team, 2025) that is analogous to the analysis of variance (ANOVA) model used in frequentist statistics. However, the Bayesian model allows for non-normal distributions that result from the conversion of the wetness metrics to percentiles and heterogeneity of variance between metrics. Additionally, the use of priors within the model leads to more robust results in scenarios with limited data by incorporating uncertainty into model comparisons that we explore (Gelman et al., 2013). Details on the implementation of the Bayesian model are in the supplemental text S3. We contrast each metric against all the others and determine the statistical difference in posterior means, which are normally distributed, by measuring the z score (number of standard deviations) between zero and the difference distribution. A z score between -1.96 and 1.96

https://doi.org/10.5194/egusphere-2026-3513
Preprint. Discussion started: 13 July 2026

indicates that the zero-difference value is within the 95% credible interval and there is not a credible difference between the two metrics, whereas a z score outside of this range indicates a credible difference. Converting the difference distributions to z scores facilitates the interpretation of the many comparisons we perform.

2.5 Ecological region evaluation

We evaluate the performance of the different wetness metrics across CONUS and four diverse ecological regions. The ecological region analysis allows us to determine if different metrics perform differently in disparate environments. We use the level-I ecoregions dataset for our ecological regions, which segregates CONUS by broad ecological similarities as determined by geology, landforms, soil characteristics, vegetation, climate, land use, wildlife, and hydrology (Omernik and Griffith, 2014) (Figure 1). We limit the number of ecological boundaries considered to ecoregions that contain more than 100 landslides (refer to section 2.1.1). This includes the Eastern Temperate Forests (EF), Marine West Coast Forest (MWCF), Mediterranean California (MC), and Northwestern Forested Mountains (NWFM) ecoregions, though many landslides with observed timing information are found in other ecoregions (Figure 1).

3 Results

The AWI: $k_d = 0.01$, TRI: variable, and TRI: uniform metrics show the highest mean percentiles on landslide days for all landslides over CONUS and within each ecoregion (Figure 2). Barplots showing the means of each distribution are shown in Figure S4. Examination of the posterior distributions of the metric means shows that the AWI: $k_d = 0.01$ and the TRI metrics' mean percentiles are statistically equivalent at a 95% credible interval within CONUS (Figure 3) and each ecological region analyzed (S5-S8). The SMAP+daily precip and the AWIET: $k_d = 0.01$ also perform relatively well over most regions, but they have a significantly different mean percentile value from the top-performing models over CONUS (Figure 3) and the Eastern Forests (EF) (Figure S5). The ARI metric consistently has the lowest mean percentiles. The relative performance of other metrics is inconsistent across the regions analyzed. The posterior distributions of the percentile means over Mediterranean California (MC) show that there are many metrics that perform equivalently over this region. Notwithstanding the overall better performances of the AWI: $k_d = 0.01$ and the TRI metrics over CONUS and different ecoregions, specific landslide locations may show alternative optimal metrics. Figures S9 and S10 show the wetness metric and the k_d coefficient for the AWI model with the highest percentile, respectively, for each landslide location.

https://doi.org/10.5194/egusphere-2026-3513
Preprint. Discussion started: 13 July 2026

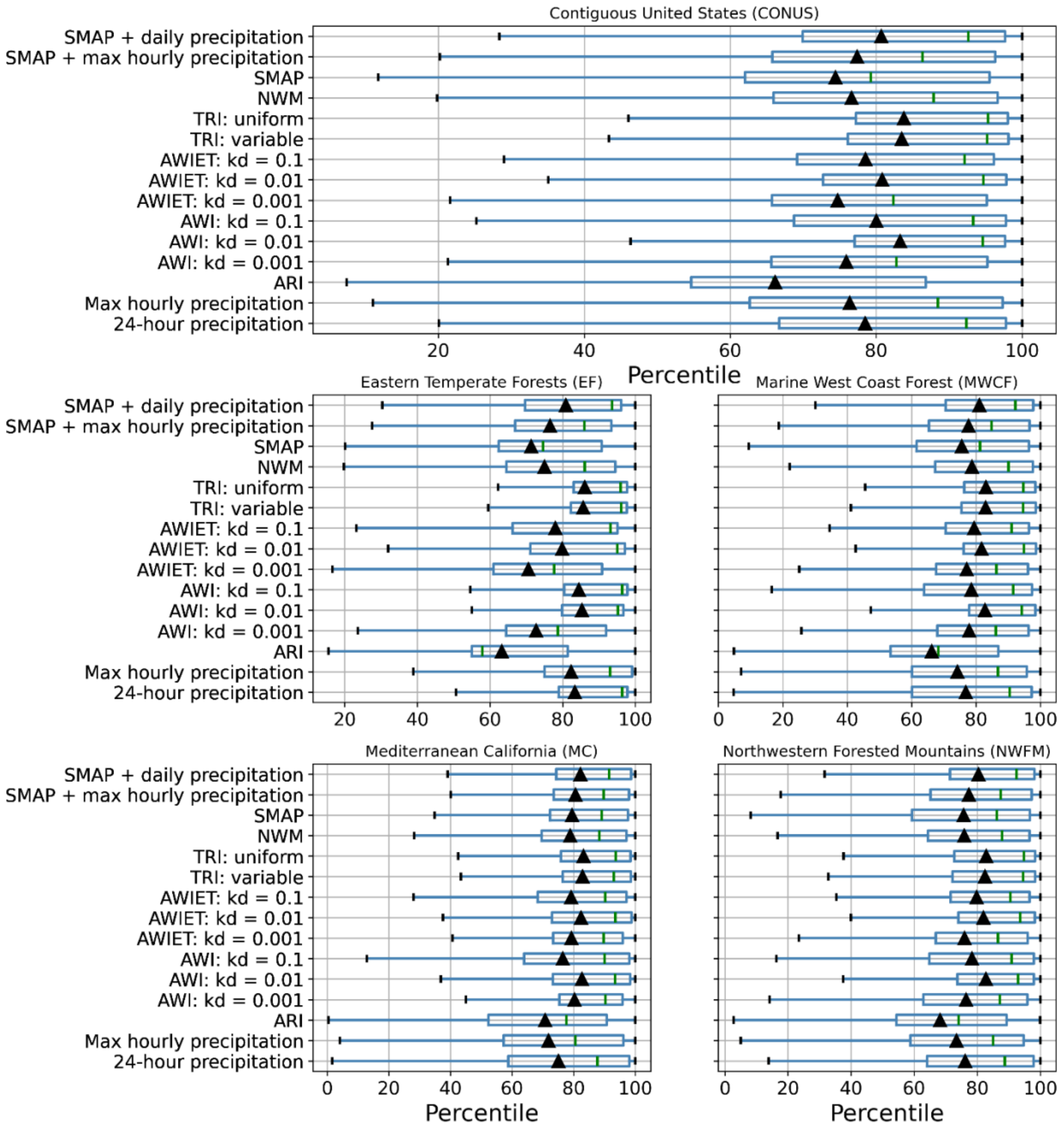

445 **Figure 2:** Boxplots of the metric values for the contiguous United States, Eastern Forests ecoregion, Mediterranean California ecoregion, Marine West Coast Forest ecoregion, and Northwestern Forested Mountains ecoregion (Omernik and Griffith, 2014). The extent of the box shows the interquartile range, the green horizontal lines show the medians, the black triangle shows the means, and the lines extending from the boxes show 1.5 times the interquartile range of the distributions. Outliers have been removed to facilitate viewing. Metric acronyms and constants are defined as follows: ARI - antecedent rainfall index; AWI - antecedent water index; kd - a drainage constant; TRI - transient rainfall index; NWM - national water model; SMAP - soil moisture active-passive.

https://doi.org/10.5194/egusphere-2026-3513
Preprint. Discussion started: 13 July 2026

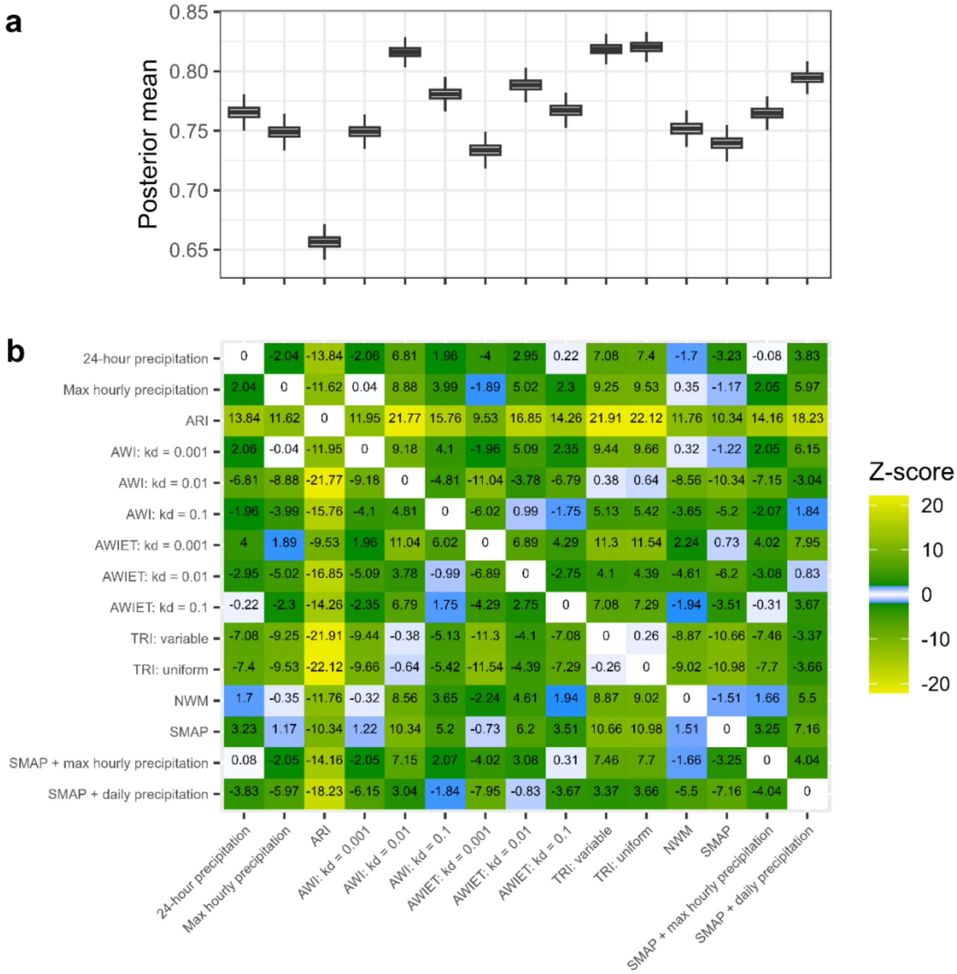

Figure 3. (a) Boxplots of the posterior means of landslide day percentiles for the different wetness metrics within the contiguous United States (CONUS). (b) z scores for an observed zero-mean posterior difference between the wetness metrics. Blue and white colors correspond to values within the 95% credible interval, indicating no credible difference, and yellow and green colors to values greater than the 95% credible interval, indicating a credible difference. The extent of the box shows the interquartile range, the horizontal lines show the medians and the lines extending from the boxes show the 1.5 times the interquartile range of the distributions. Plots for individual ecological regions are in the supplemental (Figures S5-S8). Metric acronyms and constants are defined as follows: ARI - antecedent rainfall index; AWI - antecedent water index; kd - a drainage constant; TRI - transient rainfall index; NWM - national water model; SMAP - soil moisture active-passive.

The top-performing metrics’ responses to precipitation throughout a water year (October 1 – September 30) show

https://doi.org/10.5194/egusphere-2026-3513
Preprint. Discussion started: 13 July 2026

distinct differences. Figure 4 displays a year-long time series of precipitation, SMAP + daily precipitation, TRI: variable, AWI: $k_d = 0.01$, and AWIET: $k_d = 0.01$ at three disparate point locations where a landslide has occurred (Figure 1 and S11). In this plot, the metric values are not shown as percentiles, but as values normalized by the local metric maximum. This normalization permits the comparison of multiple metrics on a shared vertical axis and preserves the metrics' behaviors. The SMAP + daily precipitation metric shows notable long and short-period changes in amplitude corresponding to the soil moisture estimates and precipitation events, respectively. The TRI: variable and AWI: $k_d = 0.01$ metrics show similar time series with exponential decays following peaks proportional to the magnitude of precipitation. The metric values accumulate if precipitation days have a high temporal frequency. In contrast, the AWIET model has a linear increase and decay until the field capacity is met (AWIET = 0). While the metric is above field capacity, the metric's response is like the TRI: variable and the AWI: $k_d = 0.01$ metrics, with a less pronounced peak and a decay only down to field capacity. At location *a* (Figure 1), many metrics perform equally well, including 24-hour precipitation and TRI: variable with a percentile of 1.0. The best metric at location b is the AWI: $k_d = 0.01$ with a percentile of 0.977. Lastly, the best metric for location c is max hourly precipitation with a percentile of 0.928.

https://doi.org/10.5194/egusphere-2026-3513
Preprint. Discussion started: 13 July 2026

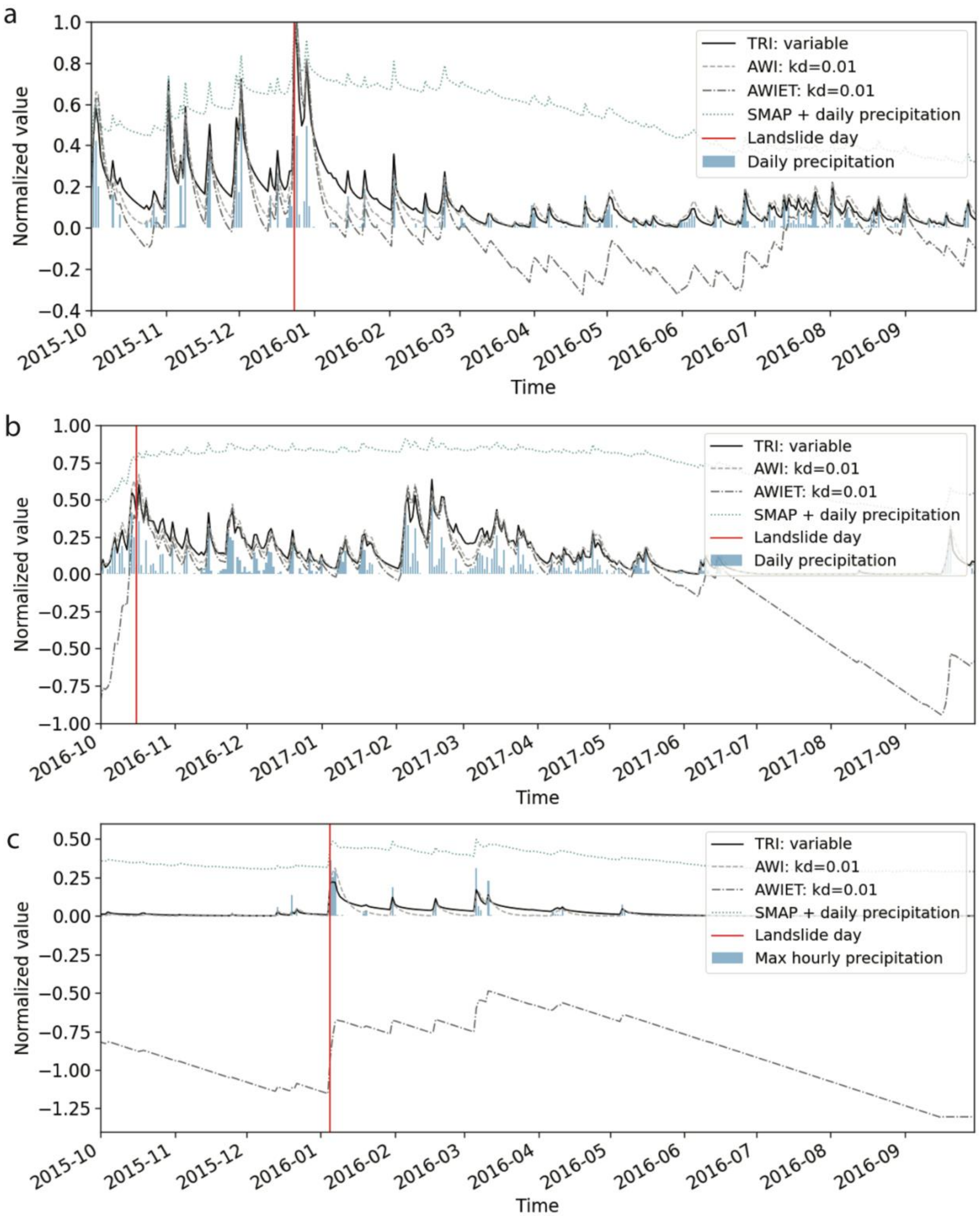

Figure 4: Water-year time series of the transient rainfall index with variable parameters (TRI: variable) (solid black), the Antecedent Water Index with a drainage constant of 0.01 h^{-1} (AWI: $k_d = 0.01$) (dashed light gray), the Antecedent Water Index with evapotranspiration and a drainage constant of 0.01 h^{-1}(AWIET: $k_d = 0.01$) (dashed

https://doi.org/10.5194/egusphere-2026-3513
Preprint. Discussion started: 13 July 2026

dark gray), and the Soil Moisture Active Passive data combined with daily precipitation estimates (SMAP + daily precipitation) (dashed teal) over (a) the eastern United States, (b) northwest United States, and (c) southern California, United States, corresponding to the landslide locations shown in Figure 1. The vertical red bar shows the timing of the local landslide day. The precipitation dataset for a and b is total daily precipitation (solid blue), and the precipitation dataset for c is maximum hourly precipitation per day (dashed blue). All metric values are normalized by the maximum value over our study period (March 31, 2015, through December 31, 2022) at the individual landslide location to facilitate visualization. Note the different scales of the vertical axes.

4 Discussion

The parsimonious leaky bucket (AWI:$k_d = 0.01$) and the transient rainfall infiltration approaches (TRI: variable, and TRI: uniform) are the best-performing metrics (Figure 2) by a statistically significant margin across diverse regions despite their ignorance of capillary flow, lateral flow, wetness-dependent drainage, and other processes that are generally considered important for local landslide assessments (Baum et al., 2008; Dietrich and Montgomery, 1998; Pack, 1998). The relatively poor performance of the wetness metrics that include some of these processes may be due to poor data constraints and the corresponding oversimplifications necessary to apply them at regional scales. Acquiring the data required for properly setting the boundary conditions and parameterizing hydrologic models that attempt to capture these processes over regional scales is not feasible at present, and may never be (Nimmo et al., 2021). The AWI and TRI metrics model the drainage immediately after an instantaneous influx of water, whereas other, more complex models do not initiate drainage until after the field capacity is met (AWIET). Consequently, the TRI and AWI metrics' relatively high correlation with landslide events may indicate that the drainage processes and their control on the accumulation of water pressure during rainfall events (Figure 4) are the most important processes to consider when assessing landslide response to precipitation over regional scales. More generally, the success of these simplified metrics highlights the effectiveness of developing new approaches designed specifically for regional hydrologic responses to precipitation that can accommodate the inherent data limitations at these scales (Hunt et al., 2013; Nimmo et al., 2021). Further development of governing principles for large-scale hydrologic and hillslope processes may lead to continued improvements in regional landslide risk reduction efforts.

The effectiveness of the AWI: k_d=0.01 and the TRI model with variable and uniform geotechnical parameters at predicting landslide days across disparate regions of the United States may reflect some common controls on soil drainage in terrain prone to catastrophic rainfall-triggered landslides. The statistically equivalent results of the TRI with uniform and variable soil parameters indicates that our tuning of the geotechnical parameters does not, on average, improve metric performance. This may partially be due to the poor constraints on these parameters at our landslide locations. It may also hint at some commonalities in the soil conditions that result in rainfall-triggered landslides across environments. Iverson (2000) showed that soils with high K_s should manifest quick and high magnitude increases in the pore water pressure that can cause rapid and catastrophic failure of the hillslope. In

https://doi.org/10.5194/egusphere-2026-3513
Preprint. Discussion started: 13 July 2026

contrast, the changes in pore water pressures in low K_s materials are more gradual, of lesser magnitude, and result in slower-moving landslides. Although Iverson's (2000) observations were based on idealized hillslopes, other studies have found that rapid shallow landslides tend to occur in areas where the shallow soils have high K_s values (Alessio, 2019; Baum et al., 2010; Qin et al., 2022; Van Asch et al., 1999; Wilson and Wieczorek, 1995). Multi-temporal landslide inventories, like the one used here, inherently have a relatively high number of rapid failure landslides compared to slow landslides, where the timing is less obvious and poorly constrained. Additionally, the curation of our landslide inventory to only include landslide events that occur on a day with a total precipitation greater than zero and a known temporal precision of a day or better means that most of the landslides analyzed in this study are likely rapid failures. It follows that we might expect our landslide locations to have high K_s values relative to most of CONUS. This hypothesis is supported by Figure 5, which shows that landslide locations generally have elevated K_s values relative to the rest of CONUS based on the first-order approximation of soil properties available from the State Soil Geographic (STATSGO) and Soil Survey Geographic (SSURGO) soil datasets. The correlation between landslide locations and K_s indicates that the TRI models and AWI:$k_d = 0.01$ perform equally well across disparate regions because they effectively characterize the higher-than-average drainage rate of soils that are conducive to rapidly failing rainfall-triggered landslides.

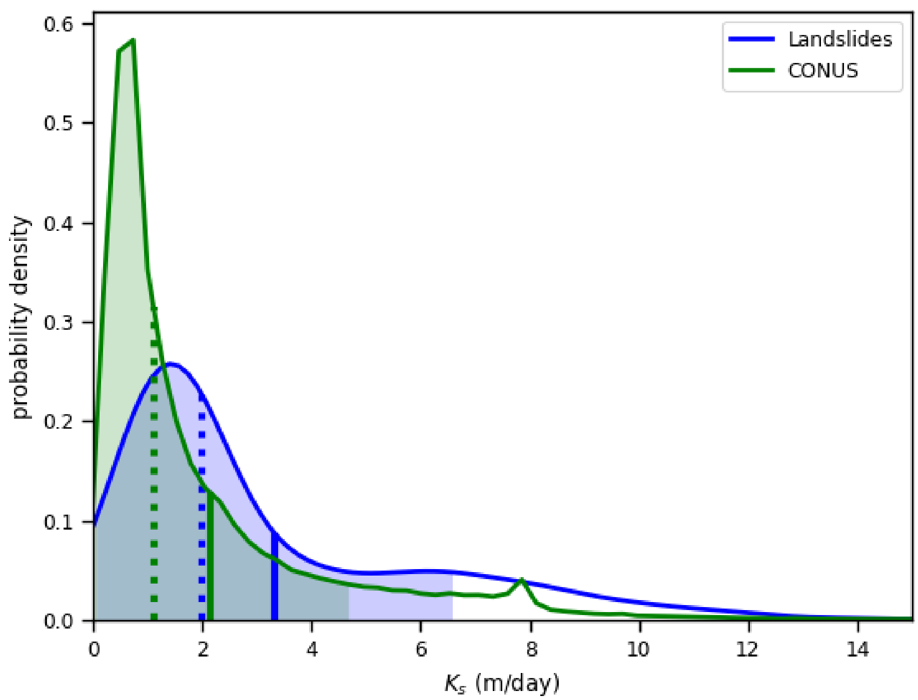

Figure 5. Kernel density plots of the estimated hydraulic conductivity (K_S) across landslide locations (blue) and all of the contiguous United States (CONUS) (green). Solid vertical lines show the means, the dashed vertical lines

https://doi.org/10.5194/egusphere-2026-3513
Preprint. Discussion started: 13 July 2026

show the medians, and the shaded regions show the standard deviations. Soil data are from the California Soil Resource Laboratory's rasterization of the Soil Survey Geographic (SSURGO) and State Soil Geographic (STATSGO) datasets (Walkinshaw et al., 2023).

We show that the AWI: $k_d = 0.01$ and TRI metrics perform best, on average, across CONUS and within different ecoregions, but local variations in performance indicate that it may not effectively capture the hydrologic effects for all landslide events. Thus, although a truly universal hydrologic metric for the prediction of rainfall-triggered landslides remains elusive, we demonstrate that simplified modeling of infiltration and storage dynamics is currently a suitable approach. Figure 6 shows the percentiles of the AWI: $k_d = 0.01$ for all the landslide days within our inventory and demonstrates that this metric performs well for most landslide events, with over 60% of the landslides having a percentile above 90%. However, there are small regions and isolated landslide locations with poor metric performances. There are a variety of explanations for why the AWI: $k_d = 0.01$ metric may not perform well over these areas. The most likely reason is that these locations have environmental conditions such as the geology, soil properties, and vegetation patterns that cause the drainage dynamics to be ineffectively captured by this metric (Ebel et al., 2008; Mirus, 2015; Pelletier et al., 2016; Richardson et al., 2019; Schmidt et al., 2001). For example, southern California shows lower percentile values compared to most other regions. Approximately 30% of these landslides are categorized as post-fire debris flows in the inventory (Belair et al., 2025). Compared to landslides in unburned areas that are triggered by infiltration of rainfall, post-fire debris flows have a fundamentally different triggering mechanism associated with enhanced runoff due to the removal of vegetation and changes to soil properties that make the soil more hydrophobic and easy to erode (McGuire et al., 2024). These attributes make recently burned areas most likely to produce landslides during short-duration (e.g., 15-minute) high-intensity rainfall events (Cavagnaro et al., 2025) and would not be effectively captured by any of the metrics analyzed here because they have a maximum temporal resolution of one hour. Other landslide types may also have unique properties that cause their hydrological conditions to not be effectively captured by the AWI $k_d = 0.01$ metric. Notwithstanding, in regional analyses where specific landslide attributes are generally lacking, the AWI $k_d = 0.01$ and TRI metrics provide a reasonable first-order estimate of landslide responses to rainfall.

https://doi.org/10.5194/egusphere-2026-3513
Preprint. Discussion started: 13 July 2026

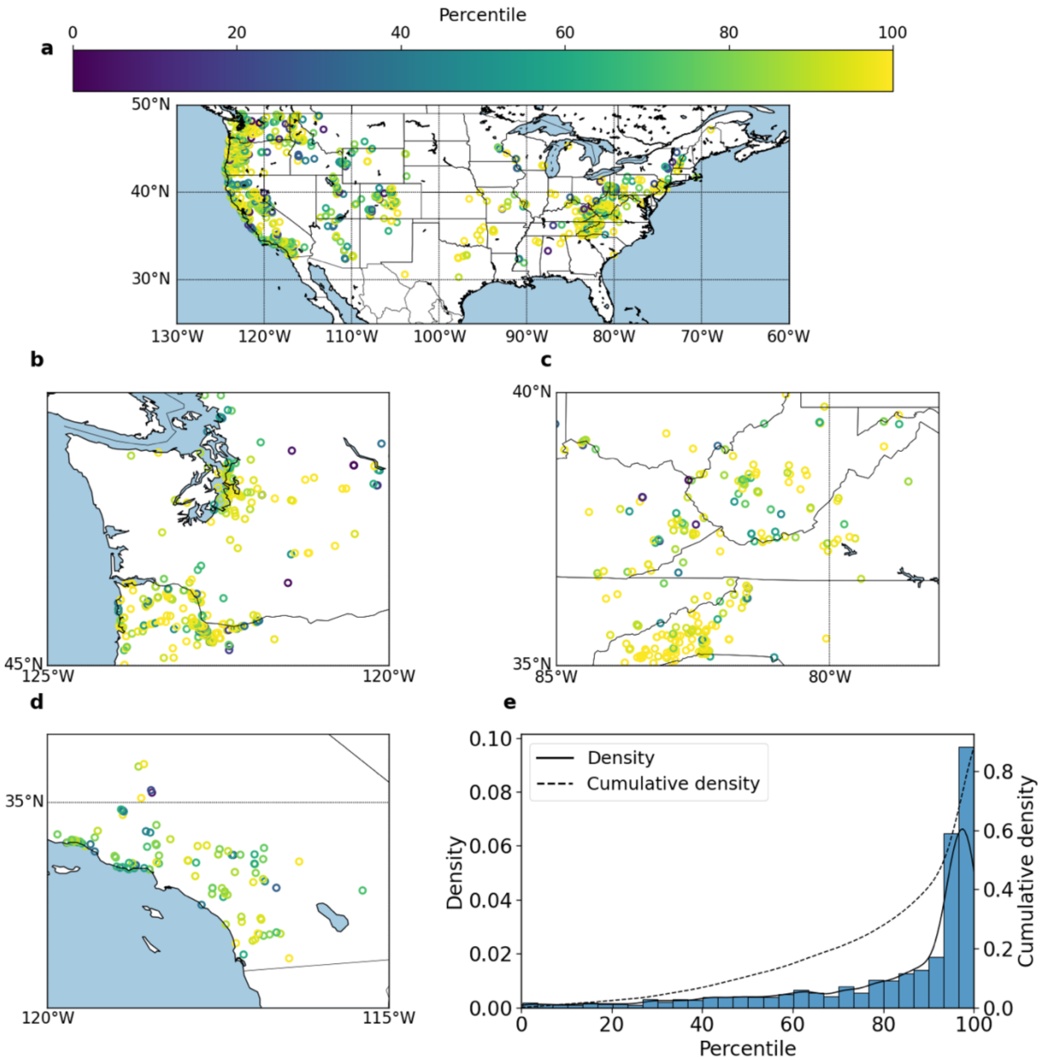

Figure 6: Spatial distribution of the antecedent water index with a drainage constant 0.01 h^{-1} (AWI: k_d = 0.01). metric percentiles of landslide days over the (a) contiguous United States, (b) northwest United States, (c) eastern United States, (d) and southern California. (e) shows the density (black line) and cumulative density (black-dashed line) of the metric across all landslides.

Local tuning of the wetness metric (Figure S9) or the AWI and TRI parameter values can help improve their performance over an area (Figure S10). This can be done by using local multi-temporal landslide inventories (Brunetti et al., 2010; Guzzetti et al., 2020; Mirus et al., 2025). However, transferring locally tuned model parameters to data-poor regions is unlikely to provide reliable results (Woodard et al., 2023) due to the inherent heterogeneity of the properties that control soil drainage and pore water pressures (Mirus, 2015). Attempts to

https://doi.org/10.5194/egusphere-2026-3513
Preprint. Discussion started: 13 July 2026

correlate the hydrologic properties of soils to other environmental factors or remotely sensed observations have proved challenging (Centeno et al., 2020; Das et al., 2010; Dongli et al., 2017; Mohanty, 2013; Zeleke and Si, 2005; Zhao et al., 2021). In contrast, the robust performance of the AWI: k_d=0.01 and TRI metrics across disparate regions indicates that they are more suitable for data-poor regions. Further studies to understand why the AWI and TRI metrics perform so well across disparate regions could leverage in situ data such as geotechnical attributes of soil, evapotranspiration rates, and weather data, coupled with ground-based measurements of pore-water pressure and soil moisture (e.g., Ebel et al., 2008; Mirus, 2015; Thomas et al., 2019). This type of analysis may also provide opportunities to refine the metrics in ways that make them more suitable for regional analysis.

Although the AWI: $k_d = 0.01$ and TRI metrics have a statistically equivalent performance, the fewer required user inputs (Table 1) and memory requirements of AWI make it our preferred wetness metric for assessing regional landslide response to precipitation. The TRI metric needs more memory due to its requirement to hold an $N \times N$ matrix in memory for the final summation (Equation 1). Additionally, the TRI metrics require estimates of saturated hydraulic conductivity and specific storage. In contrast, the AWI metric only needs an estimate of a single drainage constant, which makes it easier to parameterize by, for example, calibrating it to a landslide inventory. The simplicity of the AWI model facilitates its use in regional applications.

Our results indicate that the use of AWI:$k_d = 0.01$ metric over regional to global studies may be more effective at predicting landslide-triggering precipitation days compared to other wetness metrics. This result is similar to that of Perkins et al. (2025), who showed that a normalized bucket model with k_d=0.01 had the best performance identifying regional shallow landslide triggering conditions across California, in contrast to bucket models using other drainage constants. Our study focuses on CONUS and its ecoregions, which are geologically, topographically, and climatically diverse, with an elevation range of over 4500 m and a mean annual precipitation range of over 5500 mm (Figure 1). Although there are regions of the planet with different environmental conditions, the analyses conducted here can inform decisions on the appropriate metrics to use in other regional landslide studies. Notwithstanding, local studies that have developed metrics for assessing landslide potential are likely to be more accurate than our preferred metrics due to the accuracy and quantity of site-specific data, which can help refine the wetness metrics.

Because the AWI:$k_d = 0.01$ models' only dynamic input is precipitation, it can be used with precipitation forecasts or other low-latency precipitation datasets in landslide forecasting or early warning systems to inform risk reduction measures such as evacuations, road closures, or emergency preparedness. Recently, the LSM-based estimates of soil moisture have been used to inform different tools for landslide risk reduction (e.g., Bogaard and Greco, 2018; Felsberg et al., 2023; Palazzolo et al., 2025; Thomas et al., 2019). However, these satellite-based estimates generally have a latency of days to months (Muñoz-Sabater et al., 2021; Reichle et al., 2025), which makes them challenging for operational use in landslide early warning systems or near-real-time products (Palazzolo et al., 2025). In contrast, other wetness metrics that can use low-latency datasets generally do not perform as well as the AWI:$k_d = 0.01$

https://doi.org/10.5194/egusphere-2026-3513
Preprint. Discussion started: 13 July 2026

metric. Consequently, our results indicate better prediction of landslide-triggering rainfall conditions using the AWI metric compared to other wetness metrics commonly used for risk reduction efforts, the AWI metric can also be used with a diverse array of precipitation products that may better meet the needs for the next generation of landslide forecasting and early warning systems (Mirus et al., 2025).

Although we have curated our data and developed our statistical analysis to provide robust results, there are limitations and sources of error that are important to consider. Reporting biases towards certain specific widespread landsliding events or certain regions of the United States can artificially cause our results to favor wetness metrics that perform well over these areas or times represented in our inventory. We partially account for the spatial component of this issue by splitting CONUS into ecoregions and using the mean percentile metric to discriminate between the wetness metrics' performances. Some landslides in our inventory may have erroneous spatial or temporal data, which may also cause a misrepresentation of real failure conditions. Anthropogenic structures are not accounted for in this study and can have notable influences on the controls of landsliding that may cause different hydrologic responses compared to non-altered locations (Froude and Petley, 2018; Mirus et al., 2007; Montgomery et al., 2000). Finally, we only evaluate wetness metrics using the AORC precipitation product. Changing the precipitation dataset may change some of the results shown here. However, because the top-performing metrics performed well across diverse regions with variable infrastructure used to refine precipitation estimates, our top-performing metrics could also perform well using alternative precipitation products with similar data standards to those used in the AORC dataset (Fall et al., 2023). Finally, many other wetness metrics could be evaluated, including more complex and data-intensive approaches. However, we selected the metrics that we found to be most representative of common approaches used by researchers for assessing regional-scale landslide response to rainfall within current data limitations and availability.

5 Conclusions

We provide a systematic evaluation of a wide range of wetness metrics for characterizing the landslide response to rainfall at regional scales and find that the AWI: $k_d = 0.01$ and TRI metrics are best at differentiating landslide-triggering and non-landslide-triggering precipitation days across disparate regions of the United States. The AWI: $k_d = 0.01$ and TRI metrics have the highest mean percentiles of precipitation days for all the landslides over CONUS and within its distinct ecological regions. However, the reduced number of parameters of the AWI metric, which facilitates adapting it to different regional environments, and its computational efficiency could make it ideal for conducting regional analyses of landslide responses to precipitation. Due to the proliferation of global precipitation estimates, the AWI metric could help improve a variety of risk reduction efforts, including landslide forecasts, hazard, and risk models, and could ultimately provide the actionable information needed to reduce losses associated with rainfall-triggered landslides.

Code and data availability

The landslide data used in this analysis is available from Belair et al. (2025), the analysis of record for calibration (AORC) data are available from the U.S. National Oceanic and Atmospheric Administration (2025), the root-zone soil moisture estimates are available from Reichle et al. (2025), the evapotranspiration rates are available from Reitz et al. (2023), and the other soil parameters use in the analysis are available from Walkinshaw et al. (2023).

Supplement link

Future Link

Author contributions

JBW conceptualized, curated the data, conducted the analysis, led the investigation, developed the methodology, and prepared the manuscript. LVL assisted in the conceptualization, data curation, developing the methodology, and preparing the manuscript. BBM assisted in conceptualization, developing the methodology, and preparing the manuscript.

Acknowledgments

Any use of trade, firm, or product names is for descriptive purposes only and does not imply endorsement by the U.S. Government.

Competing interests

The authors declare no conflicts of interest relevant to this study.

References

Alessio, P.: Spatial variability of saturated hydraulic conductivity and measurement-based intensity-duration thresholds for slope stability, Santa Ynez Valley, CA, Geomorphology, 342, 103–116, https://doi.org/10.1016/j.geomorph.2019.06.004, 2019.

Baum, R. L., Savage, W. Z., and Godt, J. W.: TRIGRS — A Fortran Program for Transient Rainfall Infiltration and Grid-Based Regional Slope-Stability Analysis, Version 2.0, 2008.

https://doi.org/10.5194/egusphere-2026-3513
Preprint. Discussion started: 13 July 2026

Baum, R. L., Godt, J. W., and Savage, W. Z.: Estimating the timing and location of shallow rainfall-induced landslides using a model for transient, unsaturated infiltration, Journal of Geophysical Research: Earth Surface, 115, https://doi.org/10.1029/2009JF001321, 2010.

Beck, H. E., Pan, M., Roy, T., Weedon, G. P., Pappenberger, F., van Dijk, A. I. J. M., Huffman, G. J., Adler, R. F., and Wood, E. F.: Daily evaluation of 26 precipitation datasets using Stage-IV gauge-radar data for the CONUS, Hydrology and Earth System Sciences, 23, 207–224, https://doi.org/10.5194/hess-23-207-2019, 2019.

Belair, G. M., Jones, E. S., Luna, L. V., and Mirus, B.: Landslide inventories across the United States (3.0), https://doi.org/10.5066/P14AJF8I, 2025.

Bogaard, T. and Greco, R.: Invited perspectives: Hydrological perspectives on precipitation intensity-duration thresholds for landslide initiation: proposing hydro-meteorological thresholds, Natural Hazards and Earth System Sciences, 18, 31–39, https://doi.org/10.5194/nhess-18-31-2018, 2018.

Brunetti, M. T., Peruccacci, S., Rossi, M., Luciani, S., Valigi, D., and Guzzetti, F.: Rainfall thresholds for the possible occurrence of landslides in Italy, Natural Hazards and Earth System Sciences, 10, 447–458, https://doi.org/10.5194/nhess-10-447-2010, 2010.

Burns, W. J., Gov, Calhoun, N. C., Gov, N. C., and Gov, J. J. F.: Estimating Losses from Landslides in Oregon, presented at 3rd North American Symposium on Landslides, Roanoke, VA, June 4-8, 2017, 473–482, 2017.

Caine, N.: The rainfall intensity-duration control of shallow landslides and debris flows, Geografiska annaler: series A, physical geography, 62, 23–27, 1980.

Cavagnaro, D. B., McCoy, S. W., Thomas, M. A., Kostelnik, J., and Lindsay, D. N.: Improved Prediction of Postfire Debris Flows Through Rainfall Anomaly Maps, Geophysical Research Letters, 52, e2025GL114791, https://doi.org/10.1029/2025GL114791, 2025.

Centeno, L. N., Hu, W., Timm, L. C., She, D., da Silva Ferreira, A., Barros, W. S., Beskow, S., and Caldeira, T. L.: Dominant Control of Macroporosity on Saturated Soil Hydraulic

https://doi.org/10.5194/egusphere-2026-3513
Preprint. Discussion started: 13 July 2026

Conductivity at Multiple Scales and Locations Revealed by Wavelet Analyses, J Soil Sci Plant Nutr, 20, 1686–1702, https://doi.org/10.1007/s42729-020-00239-5, 2020.

Cosgrove, B., Gochis, D., Flowers, T., Dugger, A., Ogden, F., Graziano, T., Clark, E., Cabell, R., Casiday, N., Cui, Z., Eicher, K., Fall, G., Feng, X., Fitzgerald, K., Frazier, N., George, C., Gibbs, R., Hernandez, L., Johnson, D., Jones, R., Karsten, L., Kefelegn, H., Kitzmiller, D., Lee, H., Liu, Y., Mashriqui, H., Mattern, D., McCluskey, A., McCreight, J. L., McDaniel, R., Midekisa, A., Newman, A., Pan, L., Pham, C., RafieeiNasab, A., Rasmussen, R., Read, L., Rezaeianzadeh, M., Salas, F., Sang, D., Sampson, K., Schneider, T., Shi, Q., Sood, G., Wood, A., Wu, W., Yates, D., Yu, W., and Zhang, Y.: NOAA's National Water Model: Advancing operational hydrology through continental-scale modeling, JAWRA Journal of the American Water Resources Association, 60, 247–272, https://doi.org/10.1111/1752-1688.13184, 2024.

Crozier, M. J.: Prediction of rainfall-triggered landslides: a test of the Antecedent Water Status Model, Earth Surface Processes and Landforms, 24, 825–833, https://doi.org/10.1002/(SICI)1096-9837(199908)24:9%253C825::AID-ESP14%253E3.0.CO;2-M, 1999.

Dahal, A., Tanyas, H., van Westen, C., van der Meijde, M., Mai, P. M., Huser, R., and Lombardo, L.: Space–time landslide hazard modeling via Ensemble Neural Networks, Natural Hazards and Earth System Sciences, 24, 823–845, https://doi.org/10.5194/nhess-24-823-2024, 2024.

Das, N. N., Mohanty, B. P., and Efendiev, Y.: Characterization of effective saturated hydraulic conductivity in an agricultural field using Karhunen-Loève expansion with the Markov chain Monte Carlo technique, Water Resources Research, 46, https://doi.org/10.1029/2008WR007100, 2010.

Davis, J. and Goadrich, M.: The Relationship between Precision-Recall and ROC Curves, in: Proceedings of the 23rd International Conference on Machine Learning, New York, NY, USA, 233–240, https://doi.org/10.1145/1143844.1143874, 2006.

Dietrich, W. E. and Montgomery, D. R.: SHALSTAB: a digital terrain model for mapping shallow landslide potential, University of California, 1998.

https://doi.org/10.5194/egusphere-2026-3513
Preprint. Discussion started: 13 July 2026

Dongli, S., Qian, C., Timm, L. C., Beskow, S., Wei, H., Caldeira, T. L., and de Oliveira, L. M.: Multi-scale correlations between soil hydraulic properties and associated factors along a Brazilian watershed transect, Geoderma, 286, 15–24, https://doi.org/10.1016/j.geoderma.2016.10.017, 2017.

Du, J.: NCEP/EMC 4 Km Gridded Binary (GRIB) Stage IV Data. (1.0), https://doi. org/10.5065/D6PG1QDD, 2011.

Ebel, B. A., Loague, K., Montgomery, D. R., and Dietrich, W. E.: Physics-based continuous simulation of long-term near-surface hydrologic response for the Coos Bay experimental catchment, Water Resources Research, 44, 1–23, https://doi.org/10.1029/2007WR006442, 2008.

Emberson, R., Kirschbaum, D. B., Amatya, P., Tanyas, H., and Marc, O.: Insights from the topographic characteristics of a large global catalog of rainfall-induced landslide event inventories, Natural Hazards and Earth System Sciences, 22, 1129–1149, https://doi.org/10.5194/nhess-22-1129-2022, 2022.

Falgout, J. T., Gordon, J., Lee, L., and Williams, B.: USGS Advanced Research Computing, USGS Hovenweep Supercomputer, n.d.

Fall, G., Kitzmiller, D., Pavlovic, S., Zhang, Z., Patrick, N., St. Laurent, M., Trypaluk, C., Wu, W., and Miller, D.: The Office of Water Prediction's Analysis of Record for Calibration, version 1.1: Dataset description and precipitation evaluation, JAWRA Journal of the American Water Resources Association, 59, 1246–1272, https://doi.org/10.1111/1752-1688.13143, 2023.

Fan, X., Zhao, X., Pan, X., Liu, Y., and Liu, Y.: Investigating multiple causes of time-varying SMAP soil moisture biases based on core validation sites data, Journal of Hydrology, 612, 128151, https://doi.org/10.1016/j.jhydrol.2022.128151, 2022.

Felsberg, A., Heyvaert, Z., Poesen, J., Stanley, T., and De Lannoy, G. J. M.: Probabilistic Hydrological Estimation of LandSlides (PHELS): global ensemble landslide hazard modelling, Natural Hazards and Earth System Sciences, 23, 3805–3821, https://doi.org/10.5194/nhess-23-3805-2023, 2023.

https://doi.org/10.5194/egusphere-2026-3513
Preprint. Discussion started: 13 July 2026

Froude, M. J. and Petley, D. N.: Global fatal landslide occurrence from 2004 to 2016, Natural Hazards and Earth System Sciences, 18, 2161–2181, https://doi.org/10.5194/nhess-18-2161-2018, 2018.

Gelman, A., Carlin, J. B., Stern, H. S., Dunson, D. B., Vehtari, A., and Rubin, D. B.: Bayesian Data Analysis, Taylor & Francis, Boca Raton, 2013.

Godt, J. W., Baum, R. L., and Chleborad, A. F.: Rainfall characteristics for shallow landsliding in Seattle, Washington, USA, Earth Surface Processes and Landforms, 31, 97–110, https://doi.org/10.1002/esp.1237, 2006.

Godt, J. W., Wood, N. J., Pennaz, A. B., Mirus, B. B., Schaefer, L. N., and Slaughter, S. L.: National Strategy for Landslide Loss Reduction, U.S. Geological Survey Open-File Report 2022–1075, https://doi.org/10.3133/ofr20221075, 2022.

Guzzetti, F., Peruccacci, S., Rossi, M., and Stark, C. P.: The rainfall intensity–duration control of shallow landslides and debris flows: an update, Landslides, 5, 3–17, https://doi.org/10.1007/s10346-007-0112-1, 2008.

Guzzetti, F., Gariano, S. L., Peruccacci, S., Brunetti, M. T., Marchesini, I., Rossi, M., and Melillo, M.: Geographical landslide early warning systems, Earth-Science Reviews, 200, https://doi.org/10.1016/j.earscirev.2019.102973, 2020.

Haque, U., da Silva, P. F., Devoli, G., Pilz, J., Zhao, B., Khaloua, A., Wilopo, W., Andersen, P., Lu, P., Lee, J., Yamamoto, T., Keellings, D., Jian-Hong, W., and Glass, G. E.: The human cost of global warming: Deadly landslides and their triggers (1995–2014), Science of the Total Environment, 682, 673–684, https://doi.org/10.1016/j.scitotenv.2019.03.415, 2019.

He, H. and Ma, Y.: Imbalanced Learning - Foundations, Algorithms, and Applications, John Wiley & Sons, Inc., Hoboken, New jersey, 2013.

Hunt, A. G., Ewing, R. P., and Horton, R.: What's Wrong with Soil Physics?, Soil Science Society of America Journal, 77, 1877–1887, https://doi.org/10.2136/sssaj2013.01.0020, 2013.

https://doi.org/10.5194/egusphere-2026-3513
Preprint. Discussion started: 13 July 2026

Iverson, R. M.: Landslide triggering by rain infiltration, Water Resources Research, 36, 1897–1910, https://doi.org/10.1029/2000WR900090, 2000.

Kirschbaum, D. B. and Stanley, T.: Satellite-based assessment of rainfall-triggered landslide hazard for situational awareness, Earth's Future, 6, 505–523, https://doi.org/10.1002/2017EF000715, 2018.

Kruschke, J.: Doing Bayesian Data Analysis, Academic Press, Waltham, MA, 2015.

Lambe, T. and Whitman, R.: Soil Mechanics, John Wiley & Sons, New York, 1979.

Lin, Y. and Mitchell, K. E.: The NCEP Stage II/IV hourly precipitation analyses: development and applications, in: Paper 1.2, 19th Conference on Hydrology, San Diego, CA, 2005.

Marc, O., Stumpf, A., Malet, J. P., Gosset, M., Uchida, T., and Chiang, S. H.: Initial insights from a global database of rainfall-induced landslide inventories: The weak influence of slope and strong influence of total storm rainfall, Earth Surface Dynamics, 6, 903–922, https://doi.org/10.5194/esurf-6-903-2018, 2018.

Marc, O., Gosset, M., Saito, H., Uchida, T., and Malet, J.-P.: Spatial patterns of storm-induced landslides and their relation to rainfall anomaly maps, Geophysical Research Letters, 46, 11167–11177, https://doi.org/10.1029/2019GL083173, 2019.

Marc, O., Oliveira, R. A. J., Gosset, M., Emberson, R., and Malet, J.-P.: Global Assessment of the Capability of Satellite Precipitation Products to Retrieve Landslide-Triggering Extreme Rainfall Events, https://doi.org/10.1175/EI-D-21-0022.1, 2022.

Mason, S. J. and Graham, N. E.: Areas beneath the relative operating characteristics (ROC) and relative operating levels (ROL) curves: Statistical significance and interpretation, Quarterly Journal of the Royal Meteorological Society, 128, 2145–2166, https://doi.org/10.1256/003590002320603584, 2002.

Mathews, N. W., Leshchinsky, B. A., Mirus, B. B., Olsen, M. J., and Booth, A. M.: RegionGrow3D: A deterministic analysis for characterizing discrete three-dimensional landslide source areas on a regional scale, Journal of Geophysical Research: Earth Surface, 129, e2024JF007815, https://doi.org/10.1029/2024JF007815, 2024.

McGuire, L. A., Ebel, B. A., Rengers, F. K., Vieira, D. C. S., and Nyman, P.: Fire effects on geomorphic processes, Nat Rev Earth Environ, 5, 486–503, https://doi.org/10.1038/s43017-024-00557-7, 2024.

Milledge, D. G., Densmore, A. L., Bellugi, D., Rosser, N. J., Watt, J., Li, G., and Oven, K. J.: Simple rules to minimise exposure to coseismic landslide hazard, Natural Hazards and Earth System Sciences, 19, 837–856, https://doi.org/10.5194/nhess-19-837-2019,%202019, 2019.

Mirus, B. B.: Evaluating the importance of characterizing soil structure and horizons in parameterizing a hydrologic process model, Hydrological Processes, 29, 4611–4623, https://doi.org/10.1002/hyp.10592, 2015.

Mirus, B. B., Ebel, B. A., Loague, K., and Wemple, B. C.: Simulated effect of a forest road on near-surface hydrologic response: Redux, Earth Surface Processes and Landforms: The Journal of the British Geomorphological Research Group, 32, 126–142, https://doi.org/10.1002/esp.1387Digital%20Object%20Identifier%20(DOI), 2007.

Mirus, B. B., Becker, R. E., Baum, R. L., and Smith, J. B.: Integrating real-time subsurface hydrologic monitoring with empirical rainfall thresholds to improve landslide early warning, Landslides, 15, 1909–1919, https://doi.org/10.1007/s10346-018-0995-z, 2018.

Mirus, B. B., Jones, E. S., Baum, R. L., Godt, J. W., Slaughter, S., Crawford, M. M., Lancaster, J., Stanley, T., Kirschbaum, D. B., Burns, W. J., Schmitt, R. G., Lindsey, K. O., and McCoy, K. M.: Landslides across the USA: Occurrence, susceptibility, and data limitations, Landslides, 17, 2271–2285, https://doi.org/10.1007/s10346-020-01424-4, 2020.

Mirus, B. B., Bogaard, T., Greco, R., and Stähli, M.: Invited perspectives: Integrating hydrologic information into the next generation of landslide early warning systems, Natural Hazards and Earth System Sciences, 25, 169–182, https://doi.org/10.5194/nhess-25-169-2025, 2025.

Mohanty, B. P.: Soil Hydraulic Property Estimation Using Remote Sensing: A Review, Vadose Zone Journal, 12, vzj2013.06.0100, https://doi.org/10.2136/vzj2013.06.0100, 2013.

https://doi.org/10.5194/egusphere-2026-3513
Preprint. Discussion started: 13 July 2026

Mondini, A. C., Guzzetti, F., and Melillo, M.: Deep learning forecast of rainfall-induced shallow landslides, Nature Communications, 14, 1–10, https://doi.org/10.1038/s41467-023-38135-y, 2023.

Montgomery, D. R., Schmidt, K. M., Greenberg, H. M., and Dietrich, W. E.: Forest clearing and regional landsliding, Geology, 28, 311–314, https://doi.org/10.1130/0091-7613(2000)28%253C311:FCARL%253E2.0.CO;2, 2000.

Moreno, M., Lombardo, L., Crespi, A., Zellner, P. J., Mair, V., Pittore, M., Van Westen, C., and Steger, S.: Space-time data-driven modeling of precipitation-induced shallow landslides in South Tyrol, Italy, Science of The Total Environment, 912, 169166, https://doi.org/10.1016/j.scitotenv.2023.169166, 2024.

Muñoz-Sabater, J., Dutra, E., Agustí-Panareda, A., Albergel, C., Arduini, G., Balsamo, G., Boussetta, S., Choulga, M., Harrigan, S., Hersbach, H., Martens, B., Miralles, D. G., Piles, M., Rodríguez-Fernández, N. J., Zsoter, E., Buontempo, C., and Thépaut, J.-N.: ERA5-Land: a state-of-the-art global reanalysis dataset for land applications, Earth System Science Data, 13, 4349–4383, https://doi.org/10.5194/essd-13-4349-2021, 2021.

National Research Council: Reducing losses from landsliding in the United States, National Academies Press, Washington, https://doi.org/10.17226/19286, 1985.

Nimmo, J. R., Perkins, K. S., Plampin, M. R., Walvoord, M. A., Ebel, B. A., and Mirus, B. B.: Rapid-Response Unsaturated Zone Hydrology: Small-Scale Data, Small-Scale Theory, Big Problems, Front. Earth Sci., 9, https://doi.org/10.3389/feart.2021.613564, 2021.

NOAA: Analysis of Record for Calibration (AORC), 2025.

NOAA: NOAA National Water Model CONUS Retrospective Dataset (3.0), n.d.

Okada, K., Makihara, Y., Shimpo, A., Nagata, K., Kunitsugu, M., and Saito, H.: Soil Water Index, 47, 36–41, 2001.

https://doi.org/10.5194/egusphere-2026-3513
Preprint. Discussion started: 13 July 2026

Omernik, J. M. and Griffith, G. E.: Ecoregions of the conterminous United States: evolution of a hierarchical spatial framework, Environmental Management, 54, 1249–1266, https://doi.org/10.1007/s00267-014-0364-1, 2014.

Pack, R. T.: The SINMAP Approach to Terrain Stability Mapping, in: 8th Congress of the International Association of Engineering Geology, Vancouver, British Columbia, Canada, 1157–1166, 1998.

Palazzolo, N., Cancelliere, A., Zofei, R. D., and Peres, D. J.: Use of delayed ERA5-Land soil moisture products for improving landslide early warning, EGUsphere, 1–15, https://doi.org/10.5194/egusphere-2025-1590, 2025.

Pelletier, J. D., Broxton, P. D., Hazenberg, P., Zeng, X., Troch, P. A., Niu, G.-Y., Williams, Z., Brunke, M. A., and Gochis, D.: A gridded global data set of soil, intact regolith, and sedimentary deposit thicknesses for regional and global land surface modeling, Journal of Advances in Modeling Earth Systems, 8, 41–65, https://doi.org/10.1002/2015MS000526, 2016.

Perkins, J., Oakley, N. S., Collins, B. D., Corbett, S. C., and Burgess, W. P.: Characterizing the scale of regional landslide triggering from storm hydrometeorology, Natural Hazards and Earth System Sciences, 25, 1037–1056, https://doi.org/10.5194/nhess-25-1037-2025, 2025.

PRISM Climate Group: No Title, 2019.

Python Software Foundation: Python Language Reference, 2025.

Qin, M., Cui, P., Jiang, Y., Guo, J., Zhang, G., and Ramzan, M.: Occurrence of shallow landslides triggered by increased hydraulic conductivity due to tree roots, Landslides, 19, 2593–2604, https://doi.org/10.1007/s10346-022-01921-8, 2022.

R Core Team: R: A Language and Environment for Statistical Computing, 2025.

Reichenbach, P., Rossi, M., Malamud, B. D., Mihir, M., and Guzzetti, F.: A review of statistically-based landslide susceptibility models, Earth-Science Reviews, 180, 60–91, https://doi.org/10.1016/j.earscirev.2018.03.001, 2018.

https://doi.org/10.5194/egusphere-2026-3513
Preprint. Discussion started: 13 July 2026

Reichle, R. H., Lannoy, G. J. M. D., Liu, Q., Ardizzone, J. V., Colliander, A., Conaty, A., Crow, W., Jackson, T. J., Jones, L. A., Kimball, J. S., Koster, R. D., Mahanama, S. P., Smith, E. B., Berg, A., Bircher, S., Bosch, D., Caldwell, T. G., Cosh, M., González-Zamora, Á., Collins, C. D. H., Jensen, K. H., Livingston, S., Lopez-Baeza, E., Martínez-Fernández, J., McNairn, H., Moghaddam, M., Pacheco, A., Pellarin, T., Prueger, J., Rowlandson, T., Seyfried, M., Starks, P., Su, Z., Thibeault, M., Velde, R. van der, Walker, J., Wu, X., and Zeng, Y.: Assessment of the SMAP Level-4 Surface and Root-Zone Soil Moisture Product Using In Situ Measurements, https://doi.org/10.1175/JHM-D-17-0063.1, 2017.

Reichle, R. H., De Lannoy, G., Koster, R., Crow, W., Kimball, J., Liu, Q., and Bechtold, M.: SMAP L4 Global 3-hourly 9 km EASE-Grid Surface and Root Zone Soil Moisture Geophysical Data, Version 8, https://doi.org/10.5067/T5RUATAQREF8, 2025.

Reitz, M., Sanford, S. W., and Saxe, S. W.: Historical evapotranspiration for the conterminous U.S., https://doi.org/10.5066/P9EZ3VAS, 2023.

Richards, L. A.: Capillary conduction of liquids through porous mediums, Physics, 1, 318–333, https://doi.org/10.1063/1.1745010, 1931.

Richardson, P. W., Perron, J. T., and Schurr, N. D.: Influences of climate and life on hillslope sediment transport, Geology, 47, 423–426, https://doi.org/10.1130/G45305.1, 2019.

Saito, H. and Matsuyama, H.: Catastrophic landslide disasters triggered by record-breaking rainfall in Japan: their accurate detection with normalized soil water index in the Kii Peninsula for the year 2011, Sola, 8, 81–84, https://doi.org/10.2151/sola.2012-021, 2012.

Saito, H., Nakayama, D., and Matsuyama, H.: Relationship between the initiation of a shallow landslide and rainfall intensity—duration thresholds in Japan, Geomorphology, 118, 167–175, https://doi.org/10.1016/j.geomorph.2009.12.016, 2010.

Schmidt, K. M., Roering, J. J., Stock, J. D., Dietrich, W. E., Montgomery, D. R., and Schaub, T.: The variability of root cohesion as an influence on shallow landslide susceptibility in the Oregon Coast Range, Can. Geotech. J., 38, 995–1024, https://doi.org/10.1139/t01-031, 2001.

Schneider, D. P., Deser, C., Fasullo, J., and Trenberth, K. E.: Climate Data Guide Spurs Discovery and Understanding, Eos, Transactions American Geophysical Union, 94, 121–122, https://doi.org/10.1002/2013EO130001, 2013.

Segoni, S., Piciullo, L., and Gariano, S. L.: A review of the recent literature on rainfall thresholds for landslide occurrence, Landslides, 15, 1483–1501, https://doi.org/10.1007/s10346-018-0966-4, 2018a.

Segoni, S., Tofani, V., Rosi, A., Catani, F., and Casagli, N.: Combination of rainfall thresholds and susceptibility maps for dynamic landslide hazard assessment at regional scale, Front. Earth Sci., 6, 85, https://doi.org/10.3389/feart.2018.00085, 2018b.

Stan Development Team: Stan Reference Manual, 2025.

Stanley, T. A., Kirschbaum, D. B., Benz, G., Emberson, R. A., Amatya, P. M., Medwedeff, W., and Clark, M. K.: Data-Driven Landslide Nowcasting at the Global Scale, Frontiers in Earth Science, 9, 1–15, https://doi.org/10.3389/feart.2021.640043, 2021.

Steger, S., Moreno, M., Crespi, A., Zellner, P. J., Gariano, S. L., Brunetti, M. T., Melillo, M., Peruccacci, S., Marra, F., Kohrs, R., Goetz, J., Mair, V., and Pittore, M.: Deciphering seasonal effects of triggering and preparatory precipitation for improved shallow landslide prediction using generalized additive mixed models, Natural Hazards and Earth System Sciences Discussions, 2022, 1–38, 2022.

Thomas, M. A., Collins, B. D., and Mirus, B. B.: Assessing the feasibility of satellite-based thresholds for hydrologically driven landsliding, Water Resources Research, 55, 9006–9023, https://doi.org/10.1029/2019WR025577, 2019.

Tsunetaka, H.: Comparison of the return period for landslide-triggering rainfall events in Japan based on standardization of the rainfall period, Earth Surface Processes and Landforms, 46, 2984–2998, https://doi.org/10.1002/esp.5228, 2021.

U.S. Department of Agriculture: Soil Survey Geographic (SSURGO) Database, 2021a.

U.S. Department of Agriculture: U.S. General Soil Map (STATSGO2), 2021b.

U.S. Geological Survey: USGS EROS Archive - Digital Elevation - Global 30 Arc-Second Elevation (GTOPO30), https://doi.org//10.5066/F7DF6PQS, 2018.

Van Asch, Th. W. J., Buma, J., and Van Beek, L. P. H.: A view on some hydrological triggering systems in landslides, Geomorphology, 30, 25–32, https://doi.org/10.1016/S0169-555X(99)00042-2, 1999.

Varnes, D. J.: Slope movement types and processes, in: Landslides, Analysis and Control, Special Report 176: Transportation Research Board, National Academy of Sciences, edited by: Schuster, R. L. and Krizek, R. J., Washington DC, 11–33, 1978.

Walkinshaw, M., O'Green, A. T., and Beaudette, D. E.: Soil Properties - California Soil Resource Lab, 2023.

Wilson, R. C. and Jayko, A. S.: Preliminary maps showing rainfall thresholds for debris-flow activity, San Francisco Bay region, California, Open-File Report, U.S. Geological Survey, https://doi.org/10.3133/ofr97745F, 1997.

Wilson, R. C. and Wieczorek, G. F.: Rainfall thresholds for the initiation of debris flows at La Honda, California, Environmental & Engineering Geoscience, I, 11–27, https://doi.org/10.2113/gseegeosci.I.1.11, 1995.

Woodard, J. B. and Mirus, B. B.: Overcoming the data limitations in landslide susceptibility modeling, Science Advances, 11, eadt1541, https://doi.org/10.1126/sciadv.adt1541, 2025.

Woodard, J. B., Mirus, B. B., Crawford, M. M., Or, D., Leshchinsky, B. A., Allstadt, K. E., and Wood, N. J.: Mapping landslide susceptibility over large regions with limited data, Journal of Geophysical Research: Earth Surface, 128, e2022JF006810, https://doi.org/10.1029/2022JF006810, 2023.

Zeleke, T. B. and Si, B. C.: Scaling Relationships between Saturated Hydraulic Conductivity and Soil Physical Properties, Soil Science Society of America Journal, 69, 1691–1702, https://doi.org/10.2136/sssaj2005.0072, 2005.

https://doi.org/10.5194/egusphere-2026-3513
Preprint. Discussion started: 13 July 2026

Zhao, Y., Wang, Y., and Zhang, X.: Spatial and temporal variation in soil bulk density and saturated hydraulic conductivity and its influencing factors along a 500 km transect, CATENA, 207, 105592, https://doi.org/10.1016/j.catena.2021.105592, 2021.